

Reflection spectroscopy of spin-polarized atoms near a dielectric surface

Stefan Grafström,* Tilo Blasberg, and Dieter Suter†

Institute of Quantum Electronics, ETH Hönggerberg, CH-8093 Zürich, Switzerland

Received December 13, 1994; revised manuscript received August 7, 1995

We compare the interactions of spin-polarized Na with glass surfaces that are either bare or silicone coated. For this purpose, we reflect a laser beam that is resonant with the Na atoms from the interface, using an angle of incidence close to the critical angle of total internal reflection. Polarization-selective detection of the reflected light provides information about the ground-state orientation of the atoms, which is created by optical pumping with a second laser beam. Our theoretical description treats the atomic vapor as a homogeneous anisotropic medium characterized by a macroscopic magnetization. Comparative experimental studies performed with silicone-coated and bare glass surfaces provide evidence that wall relaxation can be observed by reflection spectroscopy. © 1996 Optical Society of America

1. INTRODUCTION

The high sensitivity and the spectral resolution of optical spectroscopy make it an ideal probe for atoms or molecules in the proximity of a solid surface. Spectroscopic data, such as the shifts of resonance frequencies or modifications of the shape, width, and strength of the resonance lines, provide information about the interaction between atoms and surfaces. A number of experiments have dealt with atoms in the gas phase, utilizing the technique of selective-reflection or evanescent-wave spectroscopy to study the interface between atomic vapors and dielectrics, which is mostly glass.^{1–4} These techniques use the resonant modification of the reflectivity by atomic transitions. The selective-reflection spectra exhibit sub-Doppler features that arise from the fact that different velocity classes contribute differently to the signal. Because of deexcitation by collisions with the surface, atoms leaving the surface show a transient behavior that results in a nonlocal response of the atomic medium to the exciting light field.^{5–8} Recently it was shown that the optical spectra are noticeably influenced by the long-range van der Waals interaction between the atoms and the surface.^{9,10}

On the other hand, atoms and molecules adsorbed on surfaces have also been studied. In particular, the quenching of the fluorescence caused by nonradiative energy transfer to metal surfaces has been investigated in a series of experiments, in which the fluorescence from dye molecules that were separated from the metal by a Langmuir–Blodgett film or a frozen noble-gas layer serving as a dielectric spacer of defined thickness¹¹ was observed. Recently experiments on Na atoms adsorbed on Langmuir–Blodgett films and self-assembled monolayers on Au and Pt surfaces were reported.^{12,13} In this case, two-photon excitation was used to suppress efficiently the background signal caused by reflection of the exciting light from the metallic substrate. It was possible to observe desorption of Na atoms from the organic film and diffusion through the film.

Optical methods have also been used to perform

magnetic-resonance spectroscopy at surfaces. As an example, Lukac and Hahn demonstrated that the reflection at the surface of a crystal containing quadrupolar nuclei changes when a radio frequency field drives the magnetic-resonance transition.¹⁴ When the radio frequency was scanned, the magnetic-resonance spectrum could be recorded. Such double-resonance methods are not the only possibility for investigating sublevel transitions. Purely optical methods can provide similar information.¹⁵ In these optical experiments, a strong circularly polarized laser beam optically pumps the atomic medium in the presence of a transverse magnetic field and creates population differences and sublevel coherences between the angular momentum substates of the electronic ground state. This order can be detected with a weak probe beam that propagates through the sample and enters a polarization-selective detector behind the sample. This method can also be applied to atoms near a dielectric surface by the reflection of the probe beam from an interface.¹⁶ The polarization of the reflected beam is again analyzed by polarization-selective detection, and the resulting signal contains information on the sublevel coherence of those atoms that are within approximately one optical wavelength of the interface. It is well known that collisions with surfaces can destroy atomic orientation,¹⁷ a phenomenon that has been studied mainly by the observation of the relaxation in the volume of the optically pumped atomic vapor, which, to a large extent, is caused by wall collisions of oriented atoms that reach the wall by diffusion.¹⁸ In contrast to these measurements, reflection of the probe beam at the surface provides local information about the atomic polarization in the immediate neighborhood of the surface.

In this paper we give a detailed discussion of the method and present experimental results. In particular, we provide a simple theoretical description of the system that allows us to calculate the signal and to analyze its dependence on various experimental parameters. The theory assumes that the medium is homogeneously polarized up to the wall, which means that spin relaxation at the wall is not taken into account. To come close to this situ-

ation experimentally and to make possible a direct comparison between theory and experiment, we performed the experiment with a silicone-coated glass surface, which is expected to cause very little relaxation. Additional measurements with a bare glass surface show characteristically different results, which indicate the presence of wall-induced spin relaxation in this case.

2. EXPERIMENTAL METHOD

A. Principle

When a light wave undergoes total internal reflection at the interface between two media with different refractive indices, an evanescent wave extends into the optically thinner medium. The component of the wave vector normal to the interface is imaginary, corresponding to an exponential decay of the electromagnetic field. For an angle of incidence θ_i near the critical angle θ_c of total internal reflection, the decay length is proportional to $\lambda/\delta^{1/2}$ with $\delta = \theta_i - \theta_c$. The optical power contained in the evanescent wave is returned to the reflected wave, which therefore carries information about optical properties, such as the refractive index and the absorption coefficient of the optically thinner medium in a surface layer whose thickness is of the order of the optical wavelength. This can be used to perform spectroscopy on atoms near a solid surface with the possibility of studying modifications of their spectroscopic properties caused by the proximity of the surface, such as the influence of wall collisions. Likewise, in the case of partial transmission, in which the angle of incidence is below the critical angle, the reflected wave is also resonantly modified by atoms in the proximity of the interface, as they contribute to the reflected beam by scattering part of the incident light.

In the experiment described in this paper, we apply this technique to the interface between Pyrex glass, either coated with silicone or bare, and Na vapor. A pump-and-probe configuration is used, in which a circularly polarized pump beam creates a ground-state polarization by optical pumping. The orientation of the atoms manifests itself as a macroscopic magnetization that makes the atomic vapor anisotropic and modifies its refractive index, making it circularly birefringent. A weak probe beam is incident upon the interface at an angle of incidence close to the critical angle of total internal reflection. The birefringence induced by the pump beam affects the polarization of the reflected probe beam, which therefore contains information about the ground-state orientation of the atoms close to the interface. This information is accessible by polarization-selective detection of the reflected beam. In the case of total reflection, the effect can be interpreted as the probe beam's penetrating into the thinner medium, traveling a distance there (the so-called Goos-Hänchen shift¹⁹), and being subjected to the birefringence, before reentering the denser medium. The Goos-Hänchen shift (together with the penetration depth of the evanescent wave) is maximum near the critical angle, so that the atomic medium is most strongly probed in this angular region. Similarly, in the situation of partial transmission, the reflected light contains a contribution reradiated by the atoms of the anisotropic medium and thus also provides information about the atomic polarization.

B. Experimental Setup

The experimental setup is shown in Fig. 1. Na vapor, together with 230-mbar Ar serving as a buffer gas, is contained in a heated glass cell that carries a glass prism on one side. The atoms near the surface of the prism are probed by a linearly polarized probe beam incident upon the interface between the prism and the atomic medium at an angle close to the critical angle of total internal reflection. The reflected light is directed onto a polarization-sensitive detector that measures the intensity difference between two orthogonally polarized components. With a half-wave plate, different orientations of linear polarizations can be selected. Insertion of a quarter-wave plate allows us alternatively to analyze the beam in terms of circularly polarized components. The atomic medium is polarized when the atoms are optically pumped with a circularly polarized pump beam derived from the same dye laser and passed through the interface at normal incidence. For this purpose, the 90° corner of the prism has been cut off. A magnetic field is applied perpendicularly to the pump beam and to the plane of incidence of the probe beam, and the polarization of the pump beam is modulated between left and right circular by means of an electro-optic modulator. This results in a forced precession of the magnetization created by optical pumping around the magnetic-field direction at the modulation frequency.²⁰ The magnitude of the precessing magnetization is resonantly enhanced if the modulation frequency is close to the Larmor frequency, as given by the strength of the magnetic field. The width of the resonance is determined by the relaxation rate of the sub-level coherence and the optical pump rate provided by the pump beam. The precession causes a modulation of the refractive index that periodically modifies the polarization of the probe beam. A lock-in amplifier allows us to extract selectively and with high sensitivity the signal caused by these variations. The angle of incidence of the probe beam can be varied over a small interval around the critical angle of total internal reflection, with a resolution of roughly 0.1 mrad, without a change in the illuminated area on the interface.

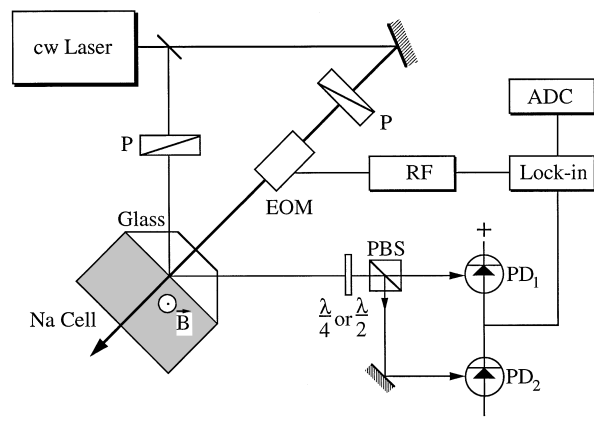


Fig. 1. Experimental setup: P's, polarizers; EOM, electro-optic modulator; RF, frequency synthesizer; ADC, analog-digital converter; $\lambda/4$ or $\lambda/2$, retardation plate; PBS, polarizing beam splitter; PD's, photodiodes.

3. THEORY

For the theoretical analysis, we describe the atomic system as a homogeneously broadened $J = 1/2 \rightarrow J' = 1/2$ transition. This description applies to the D_1 transition of Na in the presence of a buffer gas of sufficient density, which causes a pressure broadening that exceeds both the Doppler width and the hyperfine structure splittings. The polarized atomic medium may be described by the components m_x , m_y , and m_z of the magnetization vector, which are directly connected to the population difference and coherence of the ground-state Zeeman sublevels. We have shown elsewhere²¹ that a plane electromagnetic wave propagating along the z direction through such a medium can be decomposed into the two eigenpolarizations,

$$\begin{pmatrix} E_x \\ E_y \\ E_z \end{pmatrix}_{\pm} = E_0 \begin{bmatrix} 1 \\ i \left(\pm 1 + \chi_0 \frac{m_{\pm}^2}{2m_z} \right) \\ \mp \chi_0 m_{\pm} \end{bmatrix}, \quad (1)$$

where χ_0 represents the susceptibility of the unpolarized medium and $m_{\pm} = m_x \pm im_y$. The phase velocity of these two waves is characterized by the corresponding refractive indices:

$$n_{\pm} = 1 + \chi_0 \frac{1 \mp m_z}{2} \quad (2)$$

These expressions represent a first-order expansion in terms of χ_0 and provide a good approximation as long as $\chi_0 \ll 1$, a condition that is fulfilled in our experiment. Note that the refractive index is modified by only the longitudinal component of the magnetization. The eigenpolarizations are essentially left (\mathbf{E}_+) and right (\mathbf{E}_-) circular polarizations, but with a small modification if the magnetization contains a transverse component.

We now assume that a plane wave is incident at the interface between an isotropic dielectric medium on one side (refractive index n_1) and the anisotropic atomic medium on the other side (Fig. 2). Because of the birefringence of the atomic vapor, the transmitted light is split into two waves at slightly different angles θ_+ and θ_- . We restrict the discussion to angles of incidence close to the critical angle of total internal reflection, where θ_+ and θ_- are close to $\pi/2$. As long as this angular deviation is small, the transverse and the longitudinal magnetization components with respect to the directions given by θ_+ and θ_- may be approximated by the components m_x , m_y , and m_z in the fixed coordinate system defined in Fig. 2, where the z axis is oriented along the interface. Neglecting in this way the dependence of the refractive index on the propagation direction, we obtain the length of the wave vectors of the transmitted light as

$$k_{\pm} = \frac{\omega}{c} n_{\pm} = \frac{\omega}{c} \left(1 + \chi_0 \frac{1 \mp m_z}{2} \right). \quad (3)$$

Their directions θ_+ and θ_- are obtained from Snell's law:

$$\sin \theta_{\pm} = \sin \theta_i \frac{n_1}{n_{\pm}}. \quad (4)$$

We are interested primarily in the region close to the critical angle of total internal reflection. We write the

angle of incidence as $\theta_i = \theta_c + \delta$, with $\theta_c = \sin^{-1}(1/n_1)$. The transmitted beam then propagates almost parallel to the interface, and we write the angle between its \mathbf{k} vector and the surface normal as $\theta_{\pm} = \pi/2 - \delta_{\pm}$. The small angles are related by

$$\delta_{\pm}^2 = -2\delta(n_1^2 - 1)^{1/2} + \chi_0(1 \mp m_z) \quad (5)$$

to first order in δ and χ_0 . Obviously the angles δ_{\pm} are generally complex, which means that the real and the imaginary parts of the wave vector (which describe propagation and damping, respectively) are not parallel, so that the wave is inhomogeneous. In the absence of the atomic vapor, δ_{\pm} is purely imaginary for $\delta > 0$, which corresponds to total internal reflection, and purely real for $\delta < 0$ (partial transmission).

We express the electric field of the incident and the reflected waves in terms of s - and p -polarized amplitudes E_{is} , E_{ip} , E_{rs} , and E_{rp} :

$$\mathbf{E}_i = \begin{pmatrix} E_{is} \\ -E_{ip} \sin \theta_i \\ E_{ip} \cos \theta_i \end{pmatrix}, \quad \mathbf{E}_r = \begin{pmatrix} E_{rs} \\ -E_{rp} \sin \theta_i \\ -E_{rp} \cos \theta_i \end{pmatrix}, \quad (6)$$

and we write the transmitted wave as a superposition of the eigenpolarizations \mathbf{E}_{\pm} that belong to the wave vectors \mathbf{k}_+ and \mathbf{k}_- :

$$\mathbf{E}_t = t_+ \mathbf{E}_+ + t_- \mathbf{E}_-. \quad (7)$$

Equation (1) expresses the eigenpolarizations in a coordinate system in which the z axis is parallel to the wave vector, whereas in the reference frame of Fig. 2, \mathbf{k}_+ and \mathbf{k}_- deviate from the z direction by δ_{\pm} . Therefore a rotation around the x axis by δ_{\pm} has to be applied to the representation given by Eq. (1). In a linear expansion in terms of δ_{\pm} , the transmitted waves are then proportional to

$$\begin{pmatrix} E_x \\ E_y \\ E_z \end{pmatrix}_{\pm} = E_0 \begin{pmatrix} 1 \\ \pm i \\ \mp i \delta_{\pm} \end{pmatrix}. \quad (8)$$

Note that terms that contain χ_0 were omitted, as χ_0 is of second order in δ_{\pm} according to Eq. (5). The coefficients E_{is} , E_{ip} , E_{rs} , E_{rp} , and t_{\pm} are connected to each other by

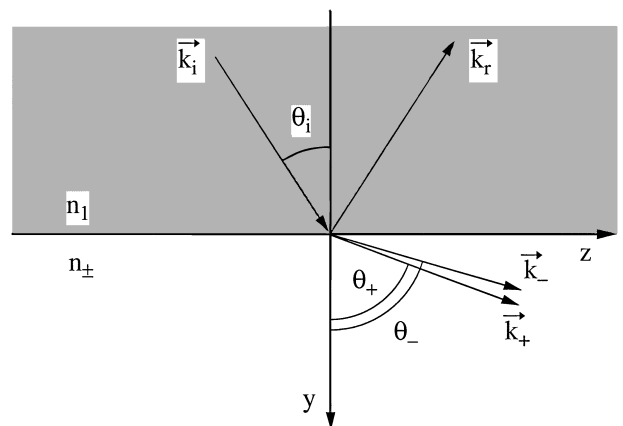


Fig. 2. Definition of the reference frame and the quantities that describe the incident, transmitted, and reflected waves.

the requirement that the electric- and the magnetic-field components E_{\parallel} and H_{\parallel} that are parallel to the interface be continuous across the boundary. For each of the four waves described by \mathbf{E}_i , \mathbf{E}_r , \mathbf{E}_+ , and \mathbf{E}_- , the magnetic field is obtained as $\mathbf{H} = (\mu_0\omega)^{-1}(\mathbf{k} \times \mathbf{E})$, where $\omega/2\pi$ denotes the frequency and \mathbf{k} is the wave vector of the respective wave. It is assumed that the magnetic permeability μ is unity in both media. The continuity conditions provide a relationship between the reflected and the incident waves that can be expressed as a reflection matrix transforming the p - and s -polarized amplitudes E_{ip} and E_{is} of the incident wave into their reflected counterparts E_{rp} and E_{rs} :

$$\begin{pmatrix} E_{rp} \\ E_{rs} \end{pmatrix} = \begin{bmatrix} r_{pp} & r_{ps} \\ r_{sp} & r_{ss} \end{bmatrix} \begin{pmatrix} E_{ip} \\ E_{is} \end{pmatrix}. \quad (9)$$

Close to the critical angle of total internal reflection the matrix assumes the following form:

$$\begin{bmatrix} r_{pp} & r_{ps} \\ r_{sp} & r_{ss} \end{bmatrix} = \begin{bmatrix} 1 & 0 \\ 0 & 1 \end{bmatrix} - \frac{1}{(n_1^2 - 1)^{1/2}} \begin{bmatrix} n_1^2\psi_+ & -in_1\psi_- \\ in_1\psi_- & \psi_+ \end{bmatrix}, \quad (10)$$

where $\psi_{\pm} = \delta_{\pm} \pm \delta_-$. In this version of the reflection matrix, only first-order contributions of δ_+ and δ_- were taken into account. In the presence of magnetization, the off-diagonal elements are nonzero so that an s -polarized incident wave does not remain s -polarized on reflection but is partially transformed into a p -polarized wave and vice versa.

We can extract the information about the magnetization from the reflected beam by splitting it into two differently polarized components and measuring their intensity difference. For a given incident polarization, the reflection matrix provides the vector $\mathbf{R} = (E_{rp}, E_{rs})$, which consists of the p - and the s -polarized components of the reflected field. The polarizing beam splitter, together with the retardation plate in front of it (see Section 2), defines two polarizations, which can be expressed as two mutually orthogonal complex unit vectors e_1 and e_2 . The detection system projects \mathbf{R} onto e_1 and e_2 and measures the intensity difference $\Delta I = |\mathbf{R} \cdot e_1|^2 - |\mathbf{R} \cdot e_2|^2$ of the

projections. As an example, we assume that the incident wave with amplitude E_0 is s polarized and that linear polarizations at an angle of $\pm 45^\circ$ with respect to the plane of incidence are detected. Then the vectors are $\mathbf{R} = E_0(r_{ps}, r_{ss})$, $e_1 = (1/\sqrt{2}, 1/\sqrt{2})$, and $e_2 = (-1/\sqrt{2}, 1/\sqrt{2})$. To first order in δ_{\pm} , the signal then becomes $\Delta I = 2I_0 \operatorname{Re}\{r_{ps}\}$, where Re denotes the real part and I_0 is the intensity of the incident beam.

Table 1 summarizes the calculated signal for a number of possible combinations of incident polarizations and analyzer settings that represent purely differential detection schemes in which the signal vanishes at the critical angle if the atomic vapor is absent. The expressions have been normalized with respect to the incident intensity I_0 . The example discussed above corresponds to the first entry in the table.

We may rewrite these expressions by introducing the angular deviation δ of the angle of incidence from the critical angle. Close to the critical angle and under the additional condition that $|\chi_0|$ is small compared with $|\delta|$, the following approximations are obtained from Eq. (5):

$$\begin{aligned} \psi_+ &= i2^{3/2}(n_1^2 - 1)^{1/4}\delta^{1/2} - \frac{i\chi_0}{2^{1/2}(n_1^2 - 1)^{1/4}\delta^{1/2}}, \\ \psi_- &= \frac{im_z\chi_0}{2^{1/2}(n_1^2 - 1)^{1/4}\delta^{1/2}}. \end{aligned} \quad (11)$$

The condition $|\delta| \gg |\chi_0|$ excludes the small angular interval in which the birefringence results in one component of the light's being totally reflected and the other one's being partially transmitted. Note that $|\chi_0|$ is of the order of 10^{-5} in our experiment so that only a narrow interval around the critical angle is excluded. The finite divergence of the probe laser beam precludes experiments that are completely within this range.

In the experiment, we use a modulation technique in which a transverse static magnetic field in combination with polarization modulation of the pump beam causes the magnetization to precess in the yz plane at the modulation frequency. The signal is extracted with a lock-in amplifier so that only signal contributions that contain m_y or m_z are detected. The detected signal reduces to the following expression in all cases listed in Table 1:

Table 1. Theoretical Expressions that Describe the Signal Obtained by Polarization-Selective Detection of the Reflected Probe Beam for Different Combinations of Incident Polarizations and Analyzer Settings^a

Incident Polarization	Analyzer Setting	Signal $\Delta I/I_0$
s	$\pm 45^\circ$	$-\frac{2n_1}{(n_1^2 - 1)^{1/2}} \operatorname{Im}\{\psi_-\}$
s	$l-r$	$-\frac{2n_1}{(n_1^2 - 1)^{1/2}} \operatorname{Re}\{\psi_-\}$
p	$\pm 45^\circ$	$\frac{2n_1}{(n_1^2 - 1)^{1/2}} \operatorname{Im}\{\psi_-\}$
p	$l-r$	$-\frac{2n_1}{(n_1^2 - 1)^{1/2}} \operatorname{Re}\{\psi_-\}$
45°	$p-s$	$-\frac{2n_1}{(n_1^2 - 1)^{1/2}} \operatorname{Im}\{\psi_-\} - (n_1^2 - 1)^{1/2} \operatorname{Re}\{\psi_+\}$

^a s , p , and 45° refer to linear polarization perpendicular, parallel, and at 45° with respect to the plane of incidence, respectively, whereas r and l denote right and left circular polarization.

$$\frac{\Delta I_{\text{mod}}}{I_0} = \pm \frac{2^{1/2} n_1}{(n_1^2 - 1)^{3/4}} m_z \operatorname{Re} \left(\frac{\chi_0}{\delta^{1/2}} \right) \quad \text{or} \\ \pm \frac{2^{1/2} n_1}{(n_1^2 - 1)^{3/4}} m_z \operatorname{Im} \left(\frac{\chi_0}{\delta^{1/2}} \right). \quad (12)$$

Whether the experiment measures the real or the imaginary part of $\chi_0/\delta^{1/2}$ and which sign it carries depends on which combination of incident polarization and detection scheme is used. Note that the formulas are valid only in a rather narrow range of δ of roughly ± 10 mrad around zero (but with the immediate neighborhood of zero excluded, as discussed above). This is due to our expansion in terms of δ_{\pm} and to the proportionality of δ_{\pm} to $\delta^{1/2}$. The angle δ_{\pm} between the transmitted waves and the interface therefore increases rapidly with δ , leaving the range in which the first-order approximation in terms of δ_{\pm} is accurate. Hence the condition that δ must fulfill is actually $|\delta|^{1/2} \ll 1$ rather than $|\delta| \ll 1$.

As $\delta^{1/2}$ changes from imaginary to real at the critical angle, the signal is governed by absorption ($\operatorname{Im}\{\chi_0\}$) in the region of partial transmission ($\delta < 0$) and by dispersion ($\operatorname{Re}\{\chi_0\}$) in the region of total internal reflection ($\delta > 0$), or vice versa. Correspondingly, the optical line shape, i.e., the signal, as a function of the laser frequency detuning, changes from absorptive to dispersive when the angle of incidence is tuned across the critical angle.

4. EXPERIMENTAL RESULTS AND DISCUSSION

For the experiments, we used the D_1 transition of Na. At the cell temperature of ~ 540 K, the number density of the Na atoms was of the order of 10^{17} m^{-3} , as estimated from the transmissivity of the atomic sample. The number of Na atoms within the evanescent wave was roughly 10^6 . The buffer gas pressure was ~ 230 mbar, which resulted in a homogeneous linewidth of ~ 4 GHz. The pump beam had an intensity of $\sim 25\text{--}75 \text{ mW/cm}^2$, whereas the probe beam intensity was $\sim 2\text{--}4 \text{ mW/cm}^2$. The strength of the magnetic field was set to $42 \mu\text{T}$, corresponding to a Larmor frequency of ~ 300 kHz. The Earth's magnetic field was compensated for by three orthogonal pairs of Helmholtz coils.

To investigate the effect of wall collisions, we used two kinds of cells, both made of Pyrex glass. In one cell, we coated the walls with polydimethylsiloxane, whereas for the second cell, we used a bare glass surface. It is well known that certain coatings, such as paraffin and silicone, prevent spin relaxation by wall collisions to a large extent.^{17,22–24} Both cells were cleaned in an ultrasonic bath with acetone and ethanol before further processing. The following procedure was used to apply the polymer coating: $\leq 100 \mu\text{L}$ of the polymer were dissolved in ~ 40 mL of ether. The cell was washed with this solution and then baked at 240°C for several hours. Then it was rinsed first with ether and then with water and finally dried, before the Na was distilled into it.

Below we first present data obtained with the coated cell, which we expect to come closest to the situation assumed by the theory developed in the preceding paragraph, namely a homogeneous magnetization within the probed layer. On the other hand, in the case of pronounced spin relaxation at the wall, the magnetization is

expected to fall off toward the wall, as compared with the bulk, so that a gradient exists near the wall that makes the medium optically inhomogeneous. The data obtained with the uncoated cell, in which a strong wall relaxation should be present, indeed show a different behavior, as is discussed below.

To study the optical line shape, the modulation frequency of the pump beam polarization was set to the Larmor frequency and the laser frequency was scanned across the Na D_1 line. The experimental observations illustrated in Fig. 3 were made with the coated cell. The probe beam was *s* polarized, and the reflected beam was split into two components polarized at an angle of $\pm 45^\circ$ with respect to the plane of reflection. The measurement was repeated for a number of different angles of incidence close to the critical angle. In accordance with the theory, the measured signal exhibits an absorptive dependence on the laser detuning in the region of partial transmission, whereas a dispersive line shape is observed in the region of total internal reflection. The change of the line shape takes place in a narrow angular interval of a few tenths

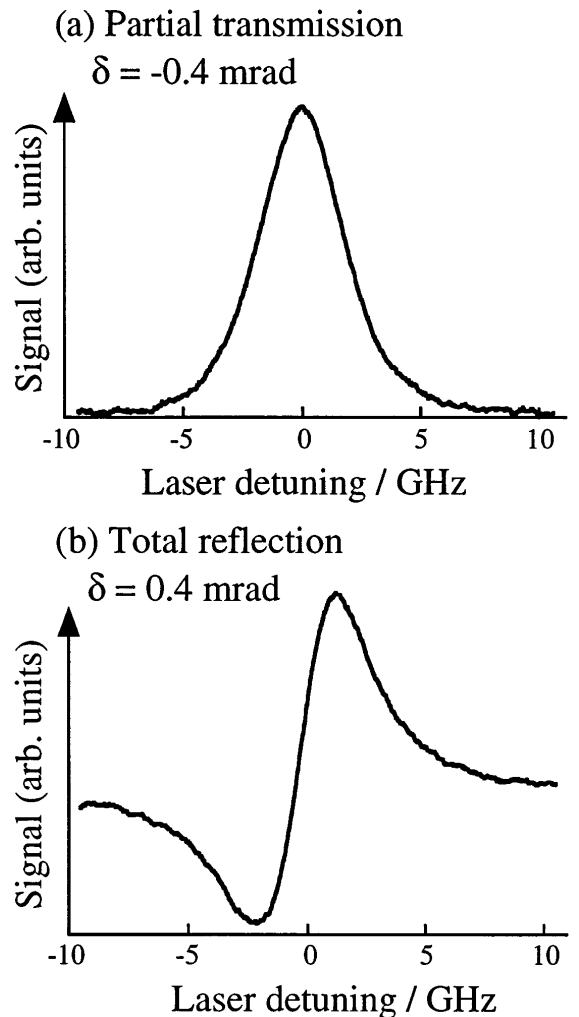


Fig. 3. Experimental spectra obtained when the laser frequency was scanned across the Na D_1 line with the pump beam polarization modulated at a constant frequency. (a) was obtained in the region of partial transmission at $\delta = -0.4$ mrad, whereas (b) resulted from a similar measurement in the range of total internal reflection at $\delta = 0.4$ mrad.

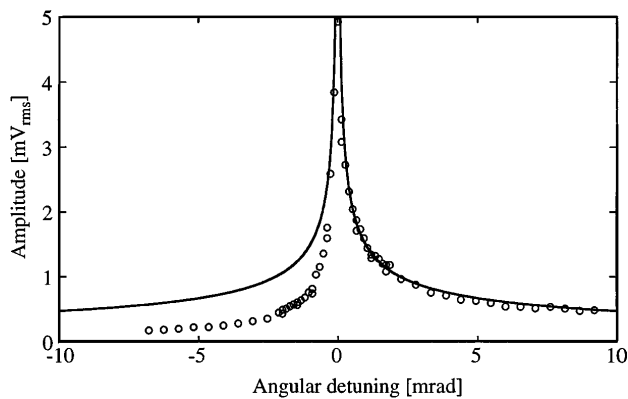


Fig. 4. Dependence of the signal amplitude on the angular detuning for the coated cell. The solid curve represent the theoretically predicted $1/|\delta|^{1/2}$ dependence.

of a milliradian, which is essentially determined by the divergence of the laser beam. Outside this interval, no dependence of the line shape on the angle of incidence was observed.

Figure 4 depicts the dependence of the signal amplitude on the angle of incidence. The angular detuning δ refers to the angular difference from the critical angle. The latter was determined experimentally by a measurement of the total reflected *s*- or *p*-polarized intensity as a function of the angle of incidence, which was found to be in excellent agreement with Fresnel's formulas. For $\delta < 0$, we used the signal maximum at the center of the absorption line as a measure of the signal amplitude, whereas for $\delta > 0$ this role was attributed to the difference between the maximum and the minimum of the dispersion line. The signal reaches its highest value at the critical angle and falls off on both sides. In the regime of total internal reflection, the experimental curve is well described by a $1/|\delta|^{1/2}$ dependence, as predicted by the theory, whereas a steeper decay is observed in the case of partial transmission. To some extent, this deviation between the experiment and the theory may be due to the fact that the first-order approximation in terms of δ_{\pm} breaks down at smaller angular detunings for partial transmission than for total reflection. This can be verified by a closer analysis of the mathematical expressions when higher-order terms are included. It is related to the fact that the influence of the higher-order corrections is different, depending on whether they are real or imaginary, and this results in an asymmetry with respect to the critical angle. In addition to the limited accuracy of the first-order approximation, there may, however, also be a physical reason for the observed deviation in the range of partial transmission: as the probe beam penetrates deeply into the atomic medium in this case, it may cause considerable damping of the magnetization, thus reducing the signal.

The magnetic-resonance line, i.e., the dependence of the signal on the frequency of the polarization modulation, is depicted in Fig. 5 (measured with the same configuration of polarizations as above). With the coated cell, we observed a narrow, near-Lorentzian line with a width of ~ 10 kHz at a pump power of 5 mW [Fig. 5(a)]. The line shape is dramatically different for the uncoated cell, as shown in Fig. 5(b). In this case, the line, which was measured with the same pump power, is clearly broadened

and has a non-Lorentzian shape characterized by wide wings. This observation is the most striking indication that strong wall relaxation is present in the uncoated cell and can be detected directly by reflection spectroscopy.

Wall relaxation should lead to a considerable reduction of the magnetization close to the wall, and this should result in a reduction of the absolute magnitude of the measured signal. A quantitative comparison of the signal amplitudes measured with the coated and the uncoated cells is depicted in Fig. 6, which is a log-log plot of the amplitudes versus the angular detuning in the regime of total internal reflection. In this case, a configuration was used in which the incident probe beam was *s* polarized and the intensity difference between the left and the right circular components of the reflected beam was measured, so that an absorptive line shape was obtained for $\delta > 0$. As calculated from the transmissivity of the samples, the number density of the Na vapor was actually higher in the experiment with the uncoated cell, but the results were rescaled to apply to the same density in both cases. As seen from Fig. 6, the signal is weaker by more than 1 order of magnitude in the case of the uncoated cell, although the pump power was higher by a factor of 3 during the measurement with the uncoated cell. This observa-

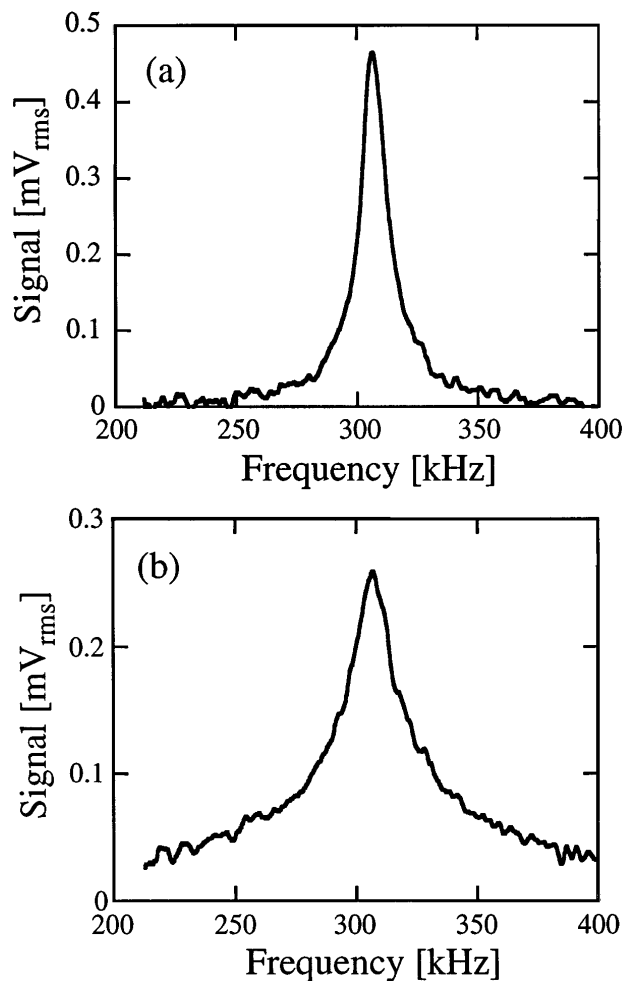


Fig. 5. Magnetic-resonance line measured at the vapor-glass interface in (a) a silicone-coated cell, (b) an uncoated cell in the regime of partial transmission. The pump beam had the same intensity in both cases.

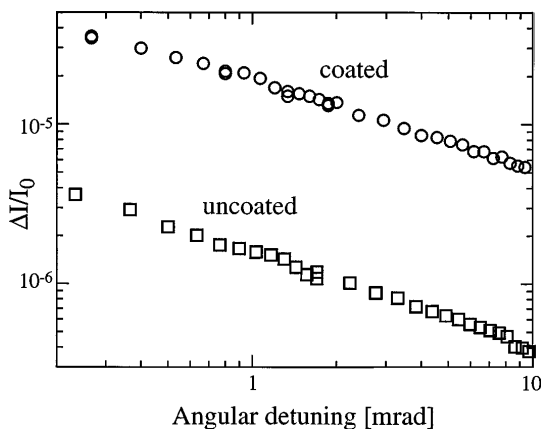


Fig. 6. Signal amplitude in the regime of total internal reflection measured with a coated cell and an uncoated cell. The pump power was 5 mW for the coated cell, but 15 mW for the uncoated cell, with the same beam diameter in both cases.

tion provides an additional confirmation that the two cells differ very much in their depolarizing properties.

As far as the optical line is concerned, we observed essentially the same line shape in both cells for total internal reflection, but characteristic differences in the regime of partial transmission. Here the data from the coated cell follow the theoretical predictions, as stated above, whereas deviations are present in the case of the bare glass surface. Near the critical angle, the line shape exhibits a pronounced asymmetry, but it comes closer to a symmetric shape for larger angular detunings of several milliradians. To clarify the possible connection between this behavior and the disorientation by wall collisions, an extension of the theory is required to include the effects of wall relaxation. In this case, the atomic medium has to be treated as inhomogeneous, because the magnetization varies as a function of the distance from the wall.

5. CONCLUSIONS

The experimental method described above represents an optically detected magnetic resonance in a thin interface layer and is characterized by a very high sensitivity, as demonstrated by the small number of atoms that contribute to the observed signal ($\sim 10^6$). The simple theory, which is based on the birefringent properties of the optically pumped atomic vapor and uses a number of approximations valid in the neighborhood of the critical angle, describes in a qualitatively correct manner the basic behavior of the system, as observed with a silicone-coated cell, in which wall relaxation, which is not taken into account by the theory, is expected to play only a minor role. In accordance with the theoretical predictions, the signal reaches its maximum at the critical angle and the optical line shape changes abruptly from absorptive to dispersive when the angle of incidence is tuned across the critical angle.

Comparative studies, including measurements with coated and uncoated glass surfaces, indicate that the strong wall relaxation caused by a bare glass surface modifies the reflection signal. Most strikingly, the magnetic-resonance line is broadened and becomes non-Lorentzian in shape. This phenomenon is accompanied by a strong decrease of the signal amplitude compared

with that of the coated cell. Also, the optical line shape is modified in that it becomes clearly asymmetric in the range of partial transmission. To describe the modified behavior theoretically, the influence of atom-surface interactions must be taken into account in a refined theory. A more detailed theory should incorporate the spin relaxation that is due to wall collisions by an extension of the theory to inhomogeneous media. With an improved theoretical understanding it should become possible to draw quantitative conclusions about the atom-surface interactions involved.

ACKNOWLEDGMENT

This research was supported by the Schweizerischer Nationalfonds and a Human Capital and Mobility grant from the Bundesamt für Bildung und Wissenschaft (contract 93.0231).

*Present address, Physikalisches Institut der Universität Heidelberg, Philosophenweg 12, D-69120 Heidelberg, Germany.

†Present address, Fachbereich Physik, Universität Dortmund, D-44221 Dortmund, Germany.

REFERENCES AND NOTES

1. S. LeBoiteux, P. Simoneau, D. Bloch, and M. Ducloy, "Doppler-free spectroscopy at a glass-vapour interface by saturated selective reflection at near normal incidence," *J. Phys. B* **20**, L149 (1987).
2. P. Simoneau, S. LeBoiteux, C. B. DeAraujo, D. Bloch, J. R. Leite, and M. Ducloy, "Doppler-free evanescent wave spectroscopy," *Opt. Commun.* **59**, 103 (1986).
3. A. M. Akul'shin, V. L. Velichanskii, A. I. Zherdev, A. S. Zibrov, V. I. Malakhova, V. V. Nikitin, V. A. Sautenkov, and G. G. Kharisov, "Selective reflection from a glass-gas interface at high angles of incidence of light," *Sov. J. Quantum Electron.* **19**, 416 (1989).
4. A. Weis, V. A. Sautenkov, and T. W. Hänsch, "Observation of ground-state Zeeman coherences in the selective reflection from cesium vapor," *Phys. Rev. A* **45**, 7991 (1992).
5. M. F. H. Schuurmans, "Spectral narrowing of selective reflection," *J. Phys.* **37**, 469 (1976).
6. A. L. J. Burgmans and J. P. Woerdman, "Selective reflection from sodium vapour at low densities," *J. Phys.* **37**, 677 (1976).
7. G. Nienhuis, F. Schuller, and M. Ducloy, "Nonlinear selective reflection from an atomic vapor at arbitrary incidence angle," *Phys. Rev. A* **38**, 5197 (1988).
8. M. Ducloy, "Influence of atom-surface collision processes in FM selective reflection spectroscopy," *Opt. Commun.* **99**, 336 (1993).
9. M. Ducloy and M. Fichet, "General theory of frequency modulated selective reflection. Influence of atom surface interactions," *J. Phys. II France* **1**, 1429 (1991).
10. M. Oria, M. Chevrollier, D. Bloch, M. Fichet, and M. Ducloy, "Spectral observation of surface-induced van der Waals attraction on atomic vapor," *Europhys. Lett.* **14**, 527 (1991).
11. D. H. Waldeck, A. P. Alivisatos, and C. B. Harris, "Nonradiative damping of molecular electronic excited states by metal surfaces," *Surf. Sci.* **158**, 103 and references therein (1985).
12. K. Bammel, J. Ellis, and H.-G. Rubahn, "Two-photon laser observation of diffusion of Na atoms through self-assembled monolayers on a Au surface," *Chem. Phys. Lett.* **201**, 101 (1993).
13. F. Balzer, K. Bammel, and H.-G. Rubahn, "Laser investigation of Na atoms deposited via inert spacer layers close to metal surfaces," *J. Chem. Phys.* **98**, 7625 (1993).
14. M. Lukac and E. L. Hahn, "External reflection and transmis-

- sion spectroscopy of $\text{Pr}^{3+}:\text{LaF}_3$ by Stark modulated optical pumping," *J. Lumin.* **42**, 257 (1988).
15. See, e.g., D. Suter and J. Mlynek, "Laser excitation and detection of magnetic resonance," in *Advances in Magnetic Resonance*, W. S. Warren, ed. (Academic, New York, 1991), Vol. 16, p. 1 and references therein.
 16. D. Suter, J. Åbersold, and J. Mlynek, "Evanescent wave spectroscopy of sublevel resonances near a glass/vapor interface," *Opt. Commun.* **84**, 269 (1991).
 17. W. Happer, "Optical pumping," *Rev. Mod. Phys.* **44**, 169 (1972).
 18. P. Bicchi, L. Moi, P. Savino, and B. Zambon, "Measurement of the diffusion coefficient of oriented Na atoms in different buffer gases," *Nuovo Cimento* **55B**, 1 (1980).
 19. A. Puri and J. L. Birman, "Goos-Hänchen beam shift at total internal reflection with application to spatially dispersive media," *J. Opt. Soc. Am. A* **3**, 543 and references therein (1986).
 20. H. Klepel and D. Suter, "Transverse optical pumping with polarization-modulated light," *Opt. Commun.* **90**, 46 (1992).
 21. D. Suter, "Propagation of light in a $J = 1/2 \leftrightarrow J' = 1/2$ resonant medium," *Opt. Commun.* **86**, 381 (1991). In the present paper, we have modified the expressions to apply to a time dependence $\exp(-i\omega t)$ rather than $\exp(i\omega t)$. This is more convenient in the case of total internal reflection, in which the z component $k_z = k_0 \cos \theta_t$ of the wave vector becomes imaginary. For a time dependence $\exp(-i\omega t)$, the imaginary part of k_z is positive for total reflection, whereas it must be negative for $\exp(i\omega t)$.
 22. M. Tanaka, T. Ohshima, K. Katori, M. Fujiwara, T. Itahashi, H. Ogata, and M. Kondo, "Depolarization of optically pumped sodium atoms by wall surfaces," *Phys. Rev. A* **41**, 1496 (1990).
 23. M. Allegrini, P. Bicchi, L. Moi, and P. Savino, "Observation of the reflection of laser oriented atoms by non disorienting surfaces," *Opt. Commun.* **32**, 396 (1980).
 24. S. I. Kanorsky, A. Weis, and J. Skalla, "A wall-collision-induced Ramsey resonance," *Appl. Phys. B* **60**, S165 (1995).